European Journal of Mechanics B/Fluids 46 (2014) 181–189

Contents lists available at ScienceDirect

European Journal of Mechanics B/Fluids

journal homepage: www.elsevier.com/locate/ejmflu

The spectrum of finite depth water waves

Benjamin Akers [a,*], David P. Nicholls [b]

[a] Air Force Institute of Technology, 2950 Hobson Way, WPAFB, OH 45433, United States
[b] University of Illinois at Chicago, 851 S. Morgan, Chicago, IL 60607, United States

ARTICLE INFO

Article history:
Received 26 October 2013
Received in revised form
20 March 2014
Accepted 22 March 2014
Available online 2 April 2014

Keywords:
Water waves
Stability
Boundary perturbation

ABSTRACT

In this contribution we study the spectrum of periodic traveling gravity waves on a two-dimensional fluid of finite depth. We extend the stable and highly accurate method of Transformed Field Expansions to the finite depth case in the presence of both simple and repeated eigenvalues, and then numerically simulate the changes in the spectrum as the wave amplitude is increased. We also calculate explicitly the first non-zero correction to the flat-water spectrum, which we observe to accurately predict the stability (or instability) for all amplitudes within the disc of analyticity of the spectrum. In addition to computations of the spectrum, we also compute the radius of the disc of analyticity of the spectrum—the amplitude boundary beyond which neither the asymptotics nor the TFE method is applicable. We observe an instability which is analytically connected to the flat state for $kh \in (0.855, 1)$.

Published by Elsevier Masson SAS.

1. Introduction

The potential flow equations arise in a wide array of fluid mechanical problems, for instance, tsunami propagation, the motion of sandbars, and pollutant transport. Traveling wave solutions of these equations have the ability to propagate energy, momentum, and passive scalars (e.g., pollutants) around the world's oceans. In this study the spectral stability of such solutions under the influence of gravity in finite depth is considered.

This problem has a rich history of both numerical and asymptotic investigations, and the *Annual Review of Fluid Mechanics* is filled with articles summarizing various aspects of the field (see [1] for a particularly relevant and well-written example). The field has roots as early as Stokes, who first expanded periodic traveling water waves as a function of the wave slope in 1845 [2], an approach which has since become commonplace (see, e.g., [3–5]).

Regarding dynamic stability of these waveforms, real progress began in the 1960s with the discovery of the Benjamin–Feir instability [6] and, of particular relevance to the current study, the amplitude expansions which led to the development of the Resonant Interaction Theory (RIT) by Phillips [7] and Benney [8] (for an excellent review of the history of RIT see [9]). In RIT, the dynamics of the solution are predicted, asymptotically in the wave slope, by equations for the amplitudes of a small set of resonantly interacting frequencies, called triad or quartet equations (based on the number of frequencies in the interaction). For traveling water waves, RIT predicts the existence and growth rates of instabilities at frequencies which satisfy such interactions. Numerical studies have computed instabilities in the neighborhood of these resonances [10–13]. In the language of these numerical studies, the even interactions (quartets, sextets, etc.) are referred to as Class I instabilities while the odd interactions (triads, quintets, etc.) are referred to as Class II instabilities. We find that an eigenvalue's dependence on amplitude is characterized by the type of resonant interaction in which the eigenfunctions' frequencies take part.

To our knowledge, all stability studies to date concerning traveling wave solutions of the full water wave problem are numerical in nature. Further, almost all of these entail the linearization of the water wave equations about a *fixed* traveling wave solution followed by the numerical approximation of the resulting eigenvalue problem. Please see the classic results of [14,15] and the more recent computations of [16–18,13] for these "Direct Numerical Simulations" (DNS) of the spectral stability problem.

By contrast to the aforementioned DNS, the authors have embarked on an investigation of spectral stability using a rather different philosophy. In short, the spectrum of the water wave operator linearized about an analytic family of traveling waves is also analytic [19,20,5] (for simple eigenvalues) so that the eigenpair (λ, w) can be expanded in the strongly convergent Taylor series

$$\lambda = \lambda(\varepsilon) = \sum_{n=0}^{\infty} \lambda_n \varepsilon^n, \qquad w = w(x;\varepsilon) = \sum_{n=0}^{\infty} w_n(x)\varepsilon^n,$$

* Corresponding author.
E-mail addresses: benjamin.akers@afit.edu (B. Akers), nicholls@math.uic.edu (D.P. Nicholls).

http://dx.doi.org/10.1016/j.euromechflu.2014.03.010
0997-7546/Published by Elsevier Masson SAS.

where ε is a wave height/slope parameter. These $\{\lambda_n, w_n\}$ have been approximated using the stable and highly (spectrally) accurate method [21] of "Transformed Field Expansions" (TFE) which was used to such great effect by one of the authors with F. Reitich [20,5] to simulate the underlying traveling waves. We refer the interested reader to [5] in particular for demonstrations of the capabilities of the TFE approach versus other Boundary Perturbation Methods including its favorable operation counts, lack of substantial numerical ill-conditioning, and applicability to *large* traveling wave profiles via numerical analytic continuation.

To put the present contribution into context we summarize our previous results:

- In [19] it was demonstrated that the spectrum of the water wave operator linearized about periodic traveling waves is *analytic* as a function of ε near simple eigenvalues.
- In [22] a TFE implementation of the theorem in [19] was used to numerically study the "evolution" of the spectrum for two-dimensional gravity waves in deep water. The role of singularities (in the Taylor series) in development of instability from the simple eigenvalue case was investigated.
- In [23] some conjectures regarding singularities in the spectrum and instability were resolved by comparing with a DNS of the spectrum in the gravity wave case.
- In [24] the TFE method was extended to include repeated eigenvalues and applied to deep-water gravity waves. RIT was used to find candidates for the "first" instabilities, those which arise at smallest wave slope.
- In [21] a rigorous numerical analysis of the TFE recursions was studied in a wide array of contexts, including the spectral stability problem.
- In [25] the TFE approach was extended to include the effect of surface tension. In deep water, triad instabilities were computed which are analytic in amplitude for fixed Bloch parameter.

In the present study we augment this line of results by:

- Extending the TFE method to the case of a fluid of finite depth.
- Computing *exactly* the first non-zero correction to the spectrum,

  $\lambda = \lambda_0 + \varepsilon^2 \lambda_2 + \cdots.$
- Predicting the amplitude of instabilities and eigenvalue collisions using second order asymptotics.
- Estimating the radius of the disc of analyticity of the spectrum $\{\lambda, w\} = \{\lambda(\varepsilon), w(x; \varepsilon)\}$ from our numerical computations.

The ultimate result, the radius of the disc of analyticity, sets our method apart from direct numerical simulations of the spectrum. This radius highlights both the strengths and weaknesses of the approach. Boundary perturbation methods are limited in applicability by their radius of convergence; the TFE method cannot compute instabilities at amplitudes larger than this radius. Although the TFE method cannot compute these large amplitude instabilities, it does provide a mechanism for detecting their location, namely at the amplitudes and Bloch parameters at which the series loses analyticity [23]. The radius also gives an upper bound for the amplitude range over which asymptotic approximations, such as those presented here, may be expected to approximate the spectrum.

It is well known that small amplitude instabilities arise from collisions of flat state eigenvalues with opposite Krein signature [10]. Our method computes such instabilities as a series in amplitude with fixed Bloch parameter. Typical instabilities occur in bands of Bloch parameters whose width grows with amplitude [12,17]. We compute finite amplitude instabilities within these bands when the bands include the resonant Bloch parameters. We also compute the locations of these bands of Bloch parameters via the radius of convergence of our amplitude expansions. Based on our results, we conclude that in order for a boundary perturbation method to compute *all* instabilities at any finite amplitude, the method must allow the Bloch parameter to vary with amplitude. If not, only very special instabilities will be computable—those which occur at the same Bloch parameter at all amplitudes. An example of such an instability is presented for $kh \in (0.855, 1)$. Small amplitude asymptotics of the spectrum of the deep-water problem with amplitude-dependent Bloch parameters are calculated in [26]; these asymptotics are consistent with the conclusions presented here.

The paper is organized as follows: in Section 2 we introduce the water wave problem, followed by the TFE method for the spectral stability problem in Section 2.1, and the concept of Bloch periodicity (Section 2.2). In Section 2.3, we discuss the computation of the leading order spectrum, which we divide into cases based on the resonant character of the repeated eigenvalue. There are no triad interactions for two-dimensional water waves without surface tension, and we begin our discussion of degenerate quartet resonances in Section 2.4, followed by non-degenerate quartet resonances in Section 2.5. In Section 3 we present our numerical results including the radius of the disc of analyticity of the spectrum, as well as a computed instability. Conclusions and future areas of research are discussed in Section 4.

2. Spectral stability of traveling water waves

In this work we apply a perturbative approach to the spectral stability problem for water waves to compute the spectrum to all orders. The leading order correction to the flat state spectrum is exactly calculated and the general order correction is computed numerically. Two independent formulations are used for these computations. The exact leading order results are calculated in a classic Taylor expansion about the mean level, similar to the models in [27,28]. For computing the general order correction, classical Boundary Perturbation Methods have been observed to be numerically unstable in certain configurations. Consequently, we have selected the Transformed Field Expansions (TFE) approach [22–24] which executes a domain-flattening change of variables before expansion. This TFE method, justified analytically in [19] and, numerically, in [21], will be briefly presented in the following sections. Unlike the aforementioned classical Boundary Perturbation algorithms, the TFE method is both strongly convergent and numerically stable.

The widely accepted model for the motion of waves on the surface of a large body of water in the absence of surface tension or viscosity are the Euler equations

$$\phi_{xx} + \phi_{zz} = 0, \quad z < \varepsilon\eta, \tag{1a}$$

$$\phi_z = 0, \quad z = -H \tag{1b}$$

$$\eta_t + \varepsilon\eta_x\phi_x = \phi_z, \quad z = \varepsilon\eta, \tag{1c}$$

$$\phi_t + \frac{\varepsilon}{2}\left(\phi_x^2 + \phi_z^2\right) + \eta = 0, \quad z = \varepsilon\eta, \tag{1d}$$

where η is the free-surface displacement and ϕ is the velocity potential. These equations describe the motion of an inviscid incompressible fluid undergoing an irrotational motion. System (1) has been non-dimensionalized as in [27,24]. We assume that the wave slope, $\varepsilon = A/L$, is small (A is a typical amplitude and L, the characteristic horizontal length, is chosen in the non-dimensionalization so that the waves have spatial period 2π). Also, the vertical dimension has been non-dimensionalized using the wavelength, so the quantity H is non-dimensional ($H = kh$). As we will later use k_j for wavenumbers of eigenfunctions, we abandon the standard notation kh in favor of simply H.

In this work, we simulate the spectrum using the TFE approach of [20,22,24,25]. To describe the TFE approach, we recall the standard (see, e.g., [24]) truncation of the water wave domain to $\{-a <$

$z < \varepsilon\eta\}$, with $-H < -a$, and the *equivalent* formulation of the governing equations (1):

$$\phi_{xx} + \phi_{zz} = 0, \quad -a < z < \varepsilon\eta, \tag{2a}$$

$$\phi_z - T[\phi] = 0, \quad z = -a, \tag{2b}$$

$$\eta_t + \varepsilon\eta_x\phi_x = \phi_z, \quad z = \varepsilon\eta, \tag{2c}$$

$$\phi_t + \frac{\varepsilon}{2}\left(\phi_x^2 + \phi_z^2\right) + \eta = 0, \quad z = \varepsilon\eta, \tag{2d}$$

where the order-one Fourier multiplier (a DNO at $y = a$) is given by

$$T[\psi(x)] = T\left[\sum_k \hat{\psi}_k e^{ikx}\right] := \sum_k |k|\tanh(|k|(H-a))\hat{\psi}_k e^{ikx};$$

here $\hat{\psi}_k$ is the k-th Fourier coefficient of $\psi(x)$

$$\psi(x) = \sum_k \hat{\psi}_k e^{ikx}.$$

2.1. Transformed field expansions

To specify the TFE recursions we consider the domain-flattening change of variables

$$x' = x, \qquad z' = a\left(\frac{z-\varepsilon\eta}{a+\varepsilon\eta}\right),$$

which are known as σ-coordinates [29] in atmospheric science and the C-method [30] in the electromagnetic theory of gratings. Defining the transformed potential

$$u(x', z') := \phi\left(x', \frac{(a+\varepsilon\eta)z'}{a} + \varepsilon\eta\right),$$

system (2) becomes, upon dropping primes,

$$u_{xx} + u_{zz} = F(x, z; u, \varepsilon\eta), \quad -a < z < 0, \tag{3a}$$

$$u_z - T[u] = J(x; u, \varepsilon\eta), \quad z = -a, \tag{3b}$$

$$\eta_t - u_z = Q(x; u, \varepsilon\eta), \quad z = 0, \tag{3c}$$

$$u_t + \eta = R(x; u, \varepsilon\eta), \quad z = 0, \tag{3d}$$

where the precise forms for F, J, Q, and R are reported in [27]. The important feature of these inhomogeneities is that if $u = \mathcal{O}(\varepsilon)$ (noting that we already have $\varepsilon\eta = \mathcal{O}(\varepsilon)$) then they are $\mathcal{O}(\varepsilon^2)$.

To study the spectral stability problem associated with solutions $(\bar{u}, \bar{\eta})$ traveling at speed c, we use the standard ansatz

$$u(x, z, t) = \bar{u}(x+ct, z) + v(x+ct, z)e^{\lambda t}$$

$$\eta(x, t) = \bar{\eta}(x+ct, z) + \zeta(x+ct)e^{\lambda t}$$

and, upon insertion into (3), quadratic products of the perturbations v and ζ are neglected. Next, the eigenvalues λ and the eigenfunctions ζ and v are also expanded as a power series in ε. Such a procedure in the Transformed Field Expansions formulation of the water wave problem yields

$$v_{n,xx} + v_{n,zz} = \tilde{F}_n(x, z), \quad -a < z < 0, \tag{4a}$$

$$v_{n,z} - Tv_n = \tilde{J}_n(x), \quad z = -a, \tag{4b}$$

$$\lambda_0\zeta_n + c_0\zeta_{n,x} - v_{n,z} = \tilde{Q}_n(x) - c_{n-1}\zeta_{1,x} - \lambda_{n-1}\zeta_1, \quad z = 0, \tag{4c}$$

$$\lambda_0 v_n + c_0 v_{n,x} + \eta_n = \tilde{R}_n(x) - c_{n-1}v_{1,x} - \lambda_{n-1}v_1, \quad z = 0. \tag{4d}$$

The exact formula for the $\tilde{F}_n, \tilde{J}_n, \tilde{Q}_n$ and $\tilde{F}_n$ appears in [22,19,23,24], and we direct the motivated reader to the (tedious) details provided therein.

2.2. Bloch periodicity

Now, a question of *fundamental* importance arises: Which boundary conditions should (v, ζ) satisfy? If, as we assume here, the traveling wave is periodic then it is natural to assume that (v, ζ) is as well. However, this restrictive (superharmonic) condition will only tell us the part of the story [14] and we need a more general class to recover instabilities (e.g., the Benjamin–Feir instability [6]) to waves of *longer* periods [15]. It is standard in these stability studies to consider Bloch (quasi) periodicity [31,32]: if $(\bar{u}, \bar{\eta})$ are periodic with respect to the lattice $\Gamma \subset \mathbf{R}^d$,

$$\bar{u}(x+\gamma, z) = \bar{u}(x, z), \qquad \bar{\eta}(x+\gamma) = \bar{\eta}(x), \quad \forall\gamma \in \Gamma,$$

then we impose the condition

$$v(x+\gamma, z) = e^{ip\cdot\gamma}v(x, z), \qquad \zeta(x+\gamma) = e^{ip\cdot\gamma}\zeta(x),$$
$$p \in \mathbf{R}^d, \ \forall\gamma \in \Gamma.$$

We note that this permits perturbations of quite general periodicities (e.g., if $d = 1$ and waves are 2π-periodic, then $p = 1/2$ permits (v, ζ) which are 4π-periodic) and even those that are *not* periodic. Fortunately, it is well-known [31] that, due to periodicity of the spectrum, it suffices to consider a bounded subset of the Bloch (quasi) periods p. For instance, for 2π-periodic functions $(d = 1)$ one only need consider the set $\{0 \le p < 1\}$ of Bloch (quasi) periods.

2.3. The leading order spectrum

To further investigate the capabilities of the TFE formulation for simulating the spectrum of the linearized water wave operator, we compute exactly the first nonzero correction to the flat state spectrum. A cubic truncation of the potential flow equations was used as a vehicle for this derivation, into which a third-order Stokes expansion was derived as in [24], yielding the traveling Stokes wave

$$\bar{\eta} = \varepsilon e^{ix} + \varepsilon^2\left(E_2 e^{2ix} + E_0\right) + \cdots + *, \tag{5a}$$

$$\bar{u} = \varepsilon\frac{i}{c_0}e^{ix} + \varepsilon^2\left(F_2 e^{2ix} + F_0\right) + \cdots + *, \tag{5b}$$

$$c = c_0 + \varepsilon c_1 + \varepsilon^2 c_2 + \cdots, \tag{5c}$$

where $*$ refers to the complex conjugate of the preceding terms. The coefficients in (5) are known, see [33,34], and have been confirmed via rederivation to be

$$c_0 = \sqrt{\tanh(H)},$$

$$c_1 = 0,$$

$$\begin{aligned} c_2 = {} & -\frac{c_0}{2\hat{\mathcal{L}}(1)^2}\left((1 - c_0^2\hat{\mathcal{L}}(1))\left(\frac{4\hat{\mathcal{L}}(1) - \hat{\mathcal{L}}(2)(\frac{3}{2}\hat{\mathcal{L}}(1)^2 - \frac{1}{2})}{\hat{\mathcal{L}}(2) - 4c_0^2}\right.\right. \\ & \left. - (\hat{\mathcal{L}}(1)^2 - 1)\right) + (4 - \hat{\mathcal{L}}(2)\hat{\mathcal{L}}(1)) \\ & \left. \times\frac{2\hat{\mathcal{L}}(1) - c_0^2(3\hat{\mathcal{L}}(1)^2 - 1)}{\hat{\mathcal{L}}(2) - 4c_0^2} - 4\hat{\mathcal{L}}(1)^2\right), \end{aligned}$$

$$E_2 = \frac{1}{\hat{\mathcal{L}}(1)(4c_0^2 - \hat{\mathcal{L}}(2))}\left(4\hat{\mathcal{L}}(1) - \hat{\mathcal{L}}(2)\left(\frac{3}{2}\hat{\mathcal{L}}(1)^2 - \frac{1}{2}\right)\right),$$

$$F_2 = \frac{1}{\hat{\mathcal{L}}(1)(4c_0^2 - \hat{\mathcal{L}}(2))}\left(\frac{2i\hat{\mathcal{L}}(1)}{c_0} - ic_0\left(3\hat{\mathcal{L}}(1)^2 - 1\right)\right),$$

$$E_0 = \frac{c_0^2}{2}\left(1 - \frac{1}{\hat{\mathcal{L}}(1)^2}\right)$$

$$F_0 = 0,$$

where $\mathcal{L}$ is the operator induced by z-derivatives on the free surface, with Fourier symbol $\hat{\mathcal{L}}(k) = |k|\tanh(|k|H)$. Notice that the traveling solution in finite depth $(H < \infty)$ has nonzero mean $E_0 \neq 0$. One could alternatively choose the potential to include a term proportional to x or t and force the mean to be zero; see [35].

The spectrum is then determined by substitution of the Stokes wave (5) and

$$\zeta = \zeta_0 + \varepsilon\zeta_1 + \varepsilon^2\zeta_2 + \cdots, \tag{6a}$$

$$v = v_0 + \varepsilon v_1 + \varepsilon^2 v_2 + \cdots, \tag{6b}$$

$$\lambda = \lambda_0 + \varepsilon\lambda_1 + \varepsilon^2\lambda_2 + \cdots, \tag{6c}$$

into the spectral stability problem, either (4) or an equivalent cubic truncation [28,24]. It is a classical calculation to show that $\lambda_0(k) = i\omega[k] - ic_0k$, where $\omega[k_j]^2 = |k_j|\tanh(H|k_j|)$. Notice that there are two choices of sign for $\omega[k]$; it need not be positive. The corrections λ_1 and λ_2 have been computed when λ_0 has multiplicity one (where ζ_0 is supported at wavenumber k_1) and when λ_0 has multiplicity two (where ζ_0 is supported at wavenumbers k_1 and k_2). When the kernel of the linear operator has dimension two, there are three cases, which we categorize by the type of resonance (using the naming convention of RIT) that occurs between the frequency of the Stokes wave $k_0 = 1$ and the frequencies of the perturbation k_1 and k_2. These cases are triads, $|k_1 - k_2| = 1$, quartets, $|k_1 - k_2| = 2$, and higher order resonances, $|k_1 - k_2| > 2$.

A quick calculation reveals that if $\lambda_0(k_1) = \lambda_0(k_2)$, then

$$\omega[k_1] - \omega[k_2] = c_0(k_1 - k_2).$$

As we consider the change in the spectrum for fixed Bloch parameter as $(\bar{u}, \bar{\eta})$ are varied, the wavenumbers of the flat state eigenfunctions are of the form $k_j = n_j + p$, with $n_j \in \mathbb{Z}$ and $p \in \mathbb{R}$. Thus the difference $k_1 - k_2 \in \mathbb{Z}$, and since $k_0 = 1$ and $\omega[k_0] = c_0$, this condition can be written as

$$k_1 - k_2 - mk_0 = 0 \qquad \text{and} \qquad \omega[k_1] - \omega[k_2] - m\omega[k_0] = 0. \tag{7}$$

Thus the existence of a flat state eigenvalue collision (i.e., repeated eigenvalues) implies the existence of a pair of frequencies which are resonant with m instances of the Stokes wave frequency k_0. Because the sign on ω is arbitrary, and ω depends only on the modulus of k, it is common to see the equations in (7) with many choices of signs, at the cost of possible redefinitions of the signs of the k_j and $\omega[k_j]$; see for example [36]. The equations in (7) describe a resonance between the Stokes wave and the perturbations, motivating our description of the spectrum based on RIT. In the following sections we observe that the finite amplitude behavior of these collisions depends critically on the value of m. For water waves without surface tension there are no triad resonances; see [25] for a discussion of triad instabilities of deep-water gravity–capillary waves. We begin the discussion of resonant instabilities with the case where the wavenumbers of the perturbations differ by two, i.e., quartets.

2.4. Degenerate quartets

When the perturbations wavenumbers do not participate in a triad interaction then $\lambda_1 = 0$ [25]. In this case, the wavenumbers are part of a quartet and the leading correction to the flat state spectrum is $\mathcal{O}(\varepsilon^2)$. Generally, finding solutions to Eq. (7) with the same Bloch parameter is non-trivial; however one can always find a quartet by setting $m = 0$,

$$k_0 - k_0 + k_1 - k_1 = 0 \quad \text{with}$$
$$\omega[k_0] - \omega[k_0] + \omega[k_1] - \omega[k_1] = 0. \tag{8}$$

We refer to this solution as a degenerate quartet, where the wavenumber at k_1 interacts with k_0 and itself. This interaction is degenerate in two senses, first it is a quartet with only two distinct wavenumbers. Second, Eq. (8) is satisfied trivially at every value of k_1. It is this interaction that determines the leading order correction to λ_0 at every simple eigenvalue, as well as at repeated eigenvalues in which the wavenumbers have difference larger than twice the Stokes wave frequency. Since the Stokes wave has $k_0 = 1$, the latter case refers to waves with $|k_2 - k_1| > 2$. These two cases have the same asymptotics because when perturbation frequencies differ by more than twice the Stokes wave frequency, they do not interact with each other to $\mathcal{O}(\varepsilon^2)$. In carrying out the asymptotics, the leading order eigenfunction, at $\mathcal{O}(1)$, is supported at k_1 and k_2. The next corrections to the eigenfunctions have predictably broader support, at $\mathcal{O}(\varepsilon)$ the wavenumbers in the correction are within $\pm k_0$ of the k_j, at $\mathcal{O}(\varepsilon^2)$ the eigenfunction has wavenumbers within $\pm 2k_0$ of the k_j, etc. At $\mathcal{O}(\varepsilon^n)$, the wavenumbers interact only if their frequency difference is less than nk_0. As a result, to $\mathcal{O}(\varepsilon^2)$, eigenvalues of multiplicity two whose frequencies differ by more than two behave as two decoupled simple eigenvalues.

For these degenerate quartets, as well as for simple eigenvalues, the leading order correction to the flat state spectrum is

$$\lambda_2 = \frac{i\omega[k_1]}{2}T_1 - \frac{1}{2}t_1, \tag{9}$$

where t_1 is the coefficient of the harmonic e^{ik_1x} in the equation for ζ_2, at $\mathcal{O}(\varepsilon^2)$, and T_1 is the coefficient of e^{ik_1x} in the equation for v_2, whose formulas are

$$\begin{aligned} t_1 &= ik_1\Bigg(c_2 + i(k_1+1)\Gamma_1^+ - \frac{\gamma_1^+}{c_0} - \frac{\gamma_1^-}{c_0} \\ &\quad + E_0 ik_1\frac{\lambda_0 + ic_0k_1}{\hat{\mathcal{L}}(k_1)} - 2\frac{\hat{\mathcal{L}}(1)}{c_0} + ik_1(\lambda_0 + ic_0k_1)\Bigg) \\ T_1 &= \Bigg(\frac{ic_2k_1(\lambda_0 + ic_0k_1)}{\hat{\mathcal{L}}(k_1)} - \frac{i(k_1+1)}{c_0}\Gamma_1^+ \\ &\quad - \frac{i\hat{\mathcal{L}}(k_1+1)\hat{\mathcal{L}}(1)}{c_0}\Gamma_1^+ + \frac{4\hat{\mathcal{L}}(1)}{c_0^2} - 2 \\ &\quad + \hat{\mathcal{L}}(k_1+1)(\lambda_0 + ic_0(k_1+1))\Gamma_1^+ - \gamma_1^+\hat{\mathcal{L}}(1) \\ &\quad - \gamma_1^-\hat{\mathcal{L}}(1) + E_0(\lambda_0 + ic_0k_1)^2 - 2\frac{ik_1(\lambda_0 + ic_0k_1)}{c_0} \\ &\quad - 2\frac{ik_1\hat{\mathcal{L}}(1)(\lambda_0 + ic_0k_1)}{c_0\hat{\mathcal{L}}(k_1)} + \frac{k_1^2(\lambda_0 + ic_0k_1)^2}{\hat{\mathcal{L}}(k_1)}\Bigg). \end{aligned}$$

The coefficients γ_j and Γ_j are the coefficients of $e^{i(k_1\pm1)x}$ in the solutions ζ_2 and v_2 respectively, with formulas

$$\begin{aligned} \begin{pmatrix} \gamma_j^\pm \\ \Gamma_j^\pm \end{pmatrix} &= \frac{1}{(\omega[k_j] \pm \omega[k_0])^2 - (\omega^2[k_j \pm k_0])} \\ &\quad \times \begin{pmatrix} i(\omega[k_j] \pm \omega[k_0])A_j^\pm + \hat{\mathcal{L}}(k_j \pm k_0)B_j^\pm \\ i(\omega[k_1] \pm \omega[k_0])B_j^\pm - A_j^\pm \end{pmatrix}, \end{aligned}$$

where the $A_j^\pm$ and $B_j^\pm$ are the projections of the forcing terms in the equations for ζ_2 and v_2 on the modes $e^{i(k_j\pm1)x}$:

$$\begin{aligned} A_j^+ &= i(k_j+1)\left(\frac{ik_j(\lambda_0 + ic_0k_j)}{\hat{\mathcal{L}}(k_j)} - \frac{1}{c_0}\right), \\ A_j^- &= i(k_j-1)\left(\frac{ik_j(\lambda_0 + ic_0k_j)}{\hat{\mathcal{L}}(k_j)} - \frac{1}{c_0}\right), \\ B_j^+ &= \left(i(\hat{\mathcal{L}}(k_j)\hat{\mathcal{L}}(1) - k_j)\frac{\lambda_0 + ic_0k_j}{c_0\hat{\mathcal{L}}(k_j)} + (\lambda_0 + ic_0k_j)^2 - \hat{\mathcal{L}}(1)\right), \\ B_j^- &= \left(i(-\hat{\mathcal{L}}(k_j)\hat{\mathcal{L}}(1) - k_j)\frac{\lambda_0 + ic_0k_j}{c_0\hat{\mathcal{L}}(k_j)} + (\lambda_0 + ic_0k_j)^2 - \hat{\mathcal{L}}(1)\right). \end{aligned}$$

Inspection of the formulae for t_1 and T_1 reveals that λ_2 in Eq. (9) is pure imaginary. Simple eigenvalues, and repeated eigenvalues whose eigenfunction's wavenumbers differ by more than two, do not lead to instability at this order of approximation in amplitude. Quintet resonances, often labeled as being between frequencies $k = p + M$ and $k = p - M - 1$ with $M = 1$, fall into this category [10,12]. With this labeling, quintets have frequency difference $2M + 1 = 5$; thus to $\mathcal{O}(\varepsilon^2)$ they do not lead to instability. Our numerical results suggest that quintet resonances have a pure imaginary spectrum throughout the disc of analyticity of the spectrum.

In previous studies, quintet instabilities have been computed, which grow in amplitude with a scaling $\mathcal{O}(\varepsilon^3)$ [12,13]. We find that quintet resonances, and those of higher order, do not generate instabilities which are analytic in amplitude for the *fixed* Bloch parameter. Instead, quintet instabilities have Bloch parameters p which vary with amplitude, ε. This phenomenon is typically reported as a movement of the bands of instability in Bloch parameter space, for example in Fig. 5 of MacKay & Saffman [10], in which we can observe that the bands of instability, at finite amplitude, do not include the resonant Bloch parameters, at zero amplitude. The need to adaptively choose the Bloch parameter as amplitude varies was more recently pointed out in [13]. Trichtchenko and Deconinck are currently pursuing a direct numerical study for water waves with surface tension which computes the location of instabilities as functions of both p and ε [37].

2.5. Quartet resonances

Quartets which may lead to instability, to $\mathcal{O}(\varepsilon^2)$, occur at repeated eigenvalues where the frequencies differ by exactly twice the Stokes wave frequency, $2k_0$,

$$k_1 - k_2 = 2k_0 \quad \text{with } \omega[k_1] + \omega[k_2] = 2\omega[k_0].$$

For these quartets, the correction to the flat state eigenvalue is determined from the root of a quadratic,

$$\lambda_2 = \frac{1}{2}(P_{2,2} + P_{1,1}) \pm \frac{1}{2}\sqrt{(P_{2,2} - P_{1,1})^2 + 4P_{1,2}P_{2,1}}, \tag{10}$$

where the $P_{i,j}$ are defined as

$$P_{1,1} = \frac{i\omega[k_1]}{2}T_1 - \frac{1}{2}t_1, \qquad P_{1,2} = \frac{i\omega[k_1]}{2}T_4 - \frac{1}{2}t_4,$$

$$P_{2,1} = \frac{i\omega[k_2]}{2}T_5 - \frac{1}{2}t_5, \qquad P_{2,2} = \frac{i\omega[k_2]}{2}T_2 - \frac{1}{2}t_2.$$

The $P_{i,j}$ are computed by enforcing solvability of the equations for ζ_3 and υ_3, i.e., the forcing terms in the equations for υ_3 and ζ_3 are orthogonal to the null space of the linear operator. The t_4, t_5 are the coefficients of the harmonics $e^{i(k_2+2)x}$ and $e^{i(k_1-2)x}$ in the equation for ζ_3, while T_4 and T_5 are the corresponding coefficients of these same harmonics in the equation for υ_3. These coefficients are

$$t_4 = i(k_2 + 2)\left(-\frac{\gamma_2^+}{c_0} + 2iF_2 + E_2\frac{\lambda_0 + ic_0k_2}{\hat{\mathcal{L}}(k_2)}ik_2 - \frac{\hat{\mathcal{L}}(1)}{c_0} + \frac{1}{2}(\lambda_0 + ic_0k_2)ik_2\right),$$

$$t_5 = i(k_1 - 2)\left(-\frac{\gamma_1^-}{c_0} - 2i\bar{F}_2 + \bar{E}_2\frac{\lambda_0 + ic_0k_1}{\hat{\mathcal{L}}(k_1)}ik_1 - \frac{\hat{\mathcal{L}}(1)}{c_0} + \frac{1}{2}(\lambda_0 + ic_0k_1)ik_1\right),$$

and

$$T_4 = \left(-\hat{\mathcal{L}}(1)\gamma_2^- - \frac{2k_2F_2(\lambda_0 + ic_0k_2)}{\hat{\mathcal{L}}(k_2)} + \hat{\mathcal{L}}(2)F_2(\lambda_0 + ic_0k_2) + E_2(\lambda_0 + ic_0k_2)^2 + 2ic_0\hat{\mathcal{L}}(2)F_2 - 1 - \frac{ik_2(\lambda_0 + ic_0k_2)}{c_0} + \frac{i(\lambda_0 + ic_0k_2)}{c_0} - \frac{ik_2\hat{\mathcal{L}}(1)(\lambda_0 + ic_0k_2)}{\hat{\mathcal{L}}(k_2)c_0} + \frac{ik_2^2\hat{\mathcal{L}}(1)(\lambda_0 + ic_0k_2)}{c_0\hat{\mathcal{L}}(k_2)} + \frac{k_2^2(\lambda_0 + ic_0k_2)^2}{2\hat{\mathcal{L}}(k_2)}\right),$$

$$T_5 = \left(-\hat{\mathcal{L}}(1)\gamma_1^- + \frac{2k_1\bar{F}_2(\lambda_0 + ic_0k_1)}{\hat{\mathcal{L}}(k_1)} + \hat{\mathcal{L}}(2)\bar{F}_2(\lambda_0 + ic_0k_1) + \bar{E}_2(\lambda_0 + ic_0k_1)^2 - 2ic_0\hat{\mathcal{L}}(2)\bar{F}_2 - 1 - \frac{ik_1(\lambda_0 + ic_0k_1)}{c_0} - \frac{i(\lambda_0 + ic_0k_1)}{c_0} - \frac{ik_1\hat{\mathcal{L}}(1)(\lambda_0 + ic_0k_1)}{\hat{\mathcal{L}}(k_1)c_0} - \frac{ik_1^2\hat{\mathcal{L}}(1)(\lambda_0 + ic_0k_1)}{c_0\hat{\mathcal{L}}(k_1)} + \frac{k_1^2(\lambda_0 + ic_0k_1)^2}{2\hat{\mathcal{L}}(k_1)}\right).$$

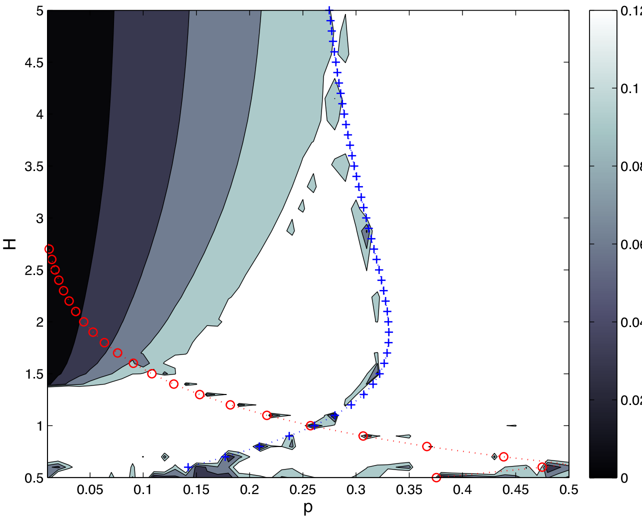

Fig. 1. The radius of the disc of analyticity (maximum allowable ε) of the spectrum is numerically estimated as a function of depth H and Bloch parameter p. The first non-canceled pole of the Padé expansion is used as an estimate of the radius, as in [24]. A quartet resonance is marked with plus signs; a quintet resonance is marked with circles. As a result of the discretization (in depth and Bloch parameter), all flat state eigenvalues are simple. The Benjamin–Feir instability causes modulational instability, and small disc of analyticity, near $p = 0$ above $H = 1.363$.

Excepting that here the formulas are more complicated, these corrections are determined by the same procedure as that in [24,25], in which the calculations of λ_2 in infinite depth appear.

Examining the coefficients in (10) reveals that the $P_{i,j}$ are pure imaginary, and thus stability is determined, to $\mathcal{O}(\varepsilon^2)$, by the discriminant in Eq. (10). We have calculated the correction λ_2 at a family of quartet resonant eigenvalues, marked by plus signs in Fig. 1, and observe instability at $\mathcal{O}(\varepsilon^2)$ only for $H \in (0.855, 1)$. The real and imaginary parts of this correction are reported in the left panel of Fig. 3.

The TFE method, employed to find the general order correction to the flat state spectrum, begins by calculating the leading order corrections based on the same solvability conditions as in the above exact calculation. At later orders, the values of λ_n are determined by linear equations, which are solvable for general n; thus, formally, a solution exists. In the next section we present the numerical results of this method, including the radius of convergence, in amplitude, of the series expansion of the eigenvalues.

3. Numerical results

In this section we summarize the results of our numerical simulations of the spectrum of finite depth gravity waves. These simulations are based on the finite depth extension of the numerical

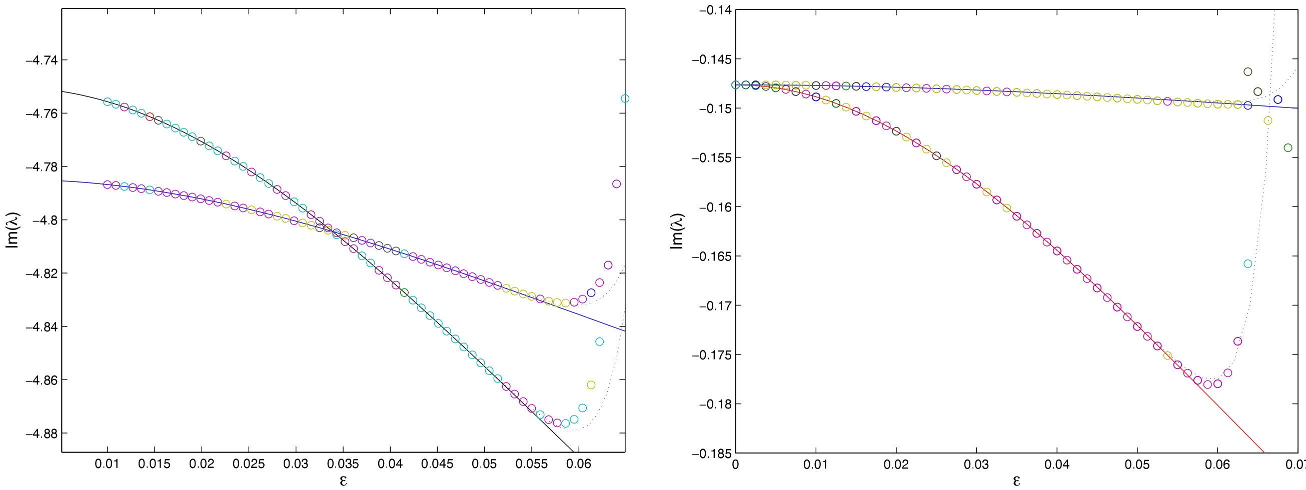

Fig. 2. The spectrum computed with the TFE method (solid curves are a Padé summation and dotted lines are the Taylor summation) at $H = 0.5$ and $p \approx 0.1065$ is compared to direct numerical simulation (DNS), marked by circles. This spectrum is pure imaginary in the neighborhood of $\varepsilon = 0$, no instability is computed within the disc of analyticity of the TFE method. At this Bloch parameter there is a finite amplitude instability near $\varepsilon = 0.05$; near this value the DNS and TFE results begin to disagree. Left: two simple eigenvalues of opposite Krein signature collide at finite amplitude. The TFE solution converges to the DNS through the first collision of these eigenvalues, a collision which leads to neither instability nor loss of analyticity. Right: a multiplicity two eigenvalue, where two opposite Krein signature eigenvalues collide at $\varepsilon = 0$, is evolved in amplitude and compared to the corresponding DNS.

method developed in [5,24,27,25]. The spectrum is computed as an analytic function of amplitude for the fixed Bloch parameter and depth. The domain of applicability of the method is examined by approximating the radius of the disc of analyticity of the spectrum. The spectrum itself is examined, with particular focus on the role of resonances in determining spectral stability. We observe that the spectrum is predominately pure imaginary; we observe a quartet-based instability only for $H \in (0.855, 1)$. This is in stark contrast to the gravity–capillary case, where analytic instabilities are common due to the existence of resonant triads [25].

Our current results suggest that there are small amplitude instabilities, for example those of [13], which our method cannot compute. These instabilities have Bloch parameters which vary with amplitude and are not analytic in amplitude for fixed Bloch parameter. In the context of the TFE method, such instabilities manifest as a radius of convergence which vanishes as it approaches a resonant Bloch parameter. Numerically computed radii with this property are depicted in Fig. 4. Thus although the TFE method cannot compute such instabilities, it can detect them in the form of a vanishing radius of convergence. When the computation of finite amplitude instabilities such as these is desired, we would advocate combining the location information from the radius of convergence of the TFE method with direct numerical simulation of the spectrum, choosing Bloch parameters only in regions where TFE did not converge. As noted in [13], the locations of instabilities in Bloch parameter space may occur at small bands of Bloch parameters, $\Delta p \approx 10^{-5}$. The radius of convergence from the TFE method can be used to design adaptive discretizations of the Bloch parameter for use in DNS simulations.

3.1. Numerical procedure

The numerical results presented here are based on a Fourier collocation in the horizontal coordinate and a Chebyshev–Tau method in the vertical. The horizontal coordinate was discretized using $N_x = 128$ points, the vertical with $N_y = 32$. The nature of both the traveling wave and the spectral data is that the nth correction to the flat state has support at wavenumbers of width $2n$. To prevent aliasing and truncation errors, when N_{stab} corrections are used, we must restrict the spectral data to those eigenpairs whose flat state eigenfunctions are supported at wavenumber $|k| < \frac{1}{2}N_x - N_{stab}$. Typical computations here use $N_{stab} = 26$, in which case the eigenpairs have flat state eigenfunctions supported at wavenumber $|k| < 51$. In Fig. 2, the results of the TFE method (lines) are compared to a traditional Direct Numerical Simulation (circles). The domain of applicability is limited by finite amplitude instabilities but not by opposite Krein signature collisions (at either finite or zero amplitude) in the left and right panels of Fig. 2 respectively.

3.2. Disc of analyticity

A novel feature of the TFE method, relative to traditional computations of the spectrum, is the ability to study the disc of analyticity of the spectrum (see Fig. 1). To generate Fig. 1, the Bloch parameter and depth were discretized. A uniform spacing in the Bloch parameter was used ($\Delta p = 0.01$) for $p \in (0, 0.5)$. For the depth, a spacing of $\Delta H = 0.1$ was used for $H \in [0.5, 2]$ and (with a larger spacing $\Delta H = 0.2125$) for $H \in (2, 5]$. For every value of p and H sampled in the plot, all of the eigenvalues in the flat state spectrum are simple. In fact, repeated eigenvalues happen on a set of measure zero: on the curves where the resonances of RIT occur. With this knowledge in mind, we have also computed the radius of the disc of analyticity in the neighborhood of these resonances with much finer samplings of the Bloch parameter (see Fig. 4). This radius was estimated using the first non-canceled pole of a Padé approximant ($N_{stab} = 26$).

The estimates of the radii reported here are in a sense overly conservative. We report the smallest ε where any eigenvalue stops being analytic. We observe that the majority of the spectrum is analytic far beyond this estimate, but report the smallest value of ε as it is the first amplitude where there may be a change in stability, as discussed in [22].

3.3. Eigenvalue collision

It is well-known that small ε instabilities occur near resonant configurations (see [1]). Moreover, instabilities arise from resonant configurations only with opposite Krein signature [10]. This necessary condition is known to be insufficient for general collisions [24,22], but is both necessary and sufficient for triads [38]. In this work we use the TFE method to analytically expand the spectrum about the flat state, including these resonant configurations. We observe that generally the spectrum is pure imaginary for the fixed Bloch parameter. Only for $H \in (0.855, 1)$ do we find an instability

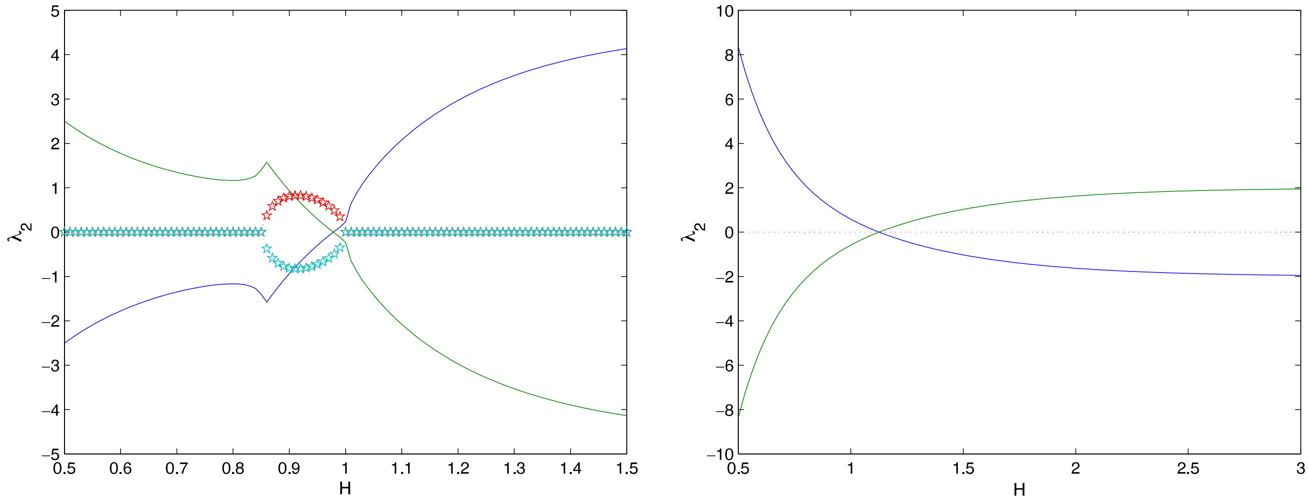

Fig. 3. Left: the first nonzero correction to the flat state spectrum, λ_2, is reported as a function of depth along a branch of quartet resonant Bloch parameters p. The real part is marked with stars, and the imaginary part with solid lines. Non-zero real parts occur for $H \in (0.855, 1)$, where a finite amplitude instability is analytically connected to the flat state. Right: the correction λ_2 is reported as a function of H along a branch of quintet resonant Bloch parameters. Bloch parameters p of the quartet and quintet resonances presented in this figure are marked, respectively, by circles and stars in Fig. 1.

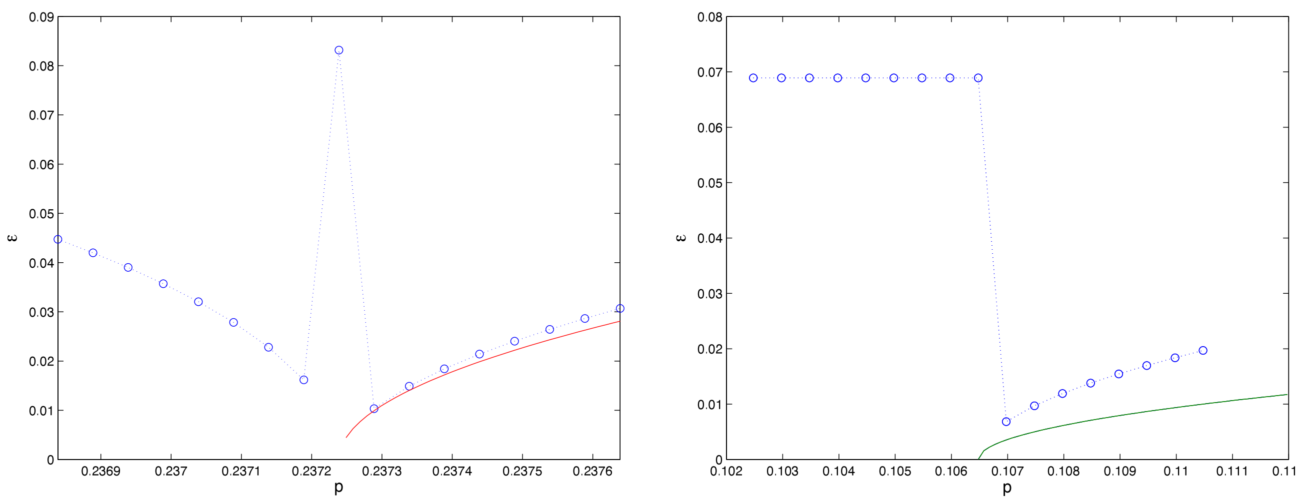

Fig. 4. The radius of the disc of analyticity of the spectrum is numerically estimated as a function of the Bloch parameter, p, near two quartet resonances. On the left, the radius of the disc of analyticity is reported at $H = 0.9$, near the quartet resonance at $\varepsilon = 0$, $\lambda_0 \approx -0.424i$, $p \approx 0.237$. At the resonant Bloch parameter, there is a real eigenvalue which is analytic in ε. We observe that the radius of the disc vanishes like the square root of the distance from the resonant Bloch parameter. The solid line marks the amplitude at which the collision occurs based on the second order asymptotics of Section 2.5. On the right, the radius is presented at $H = 0.5$ near $p \approx 0.107$. At the resonant Bloch parameter on the right panel the spectrum is pure imaginary.

which both occurs at the fixed Bloch parameter and is analytic in amplitude. On the other hand, we do observe numerical evidence of modulated instabilities, where the frequency depends on amplitude, in the neighborhood of these resonant parameters. In the context of the TFE method, these instabilities are manifested as a vanishing disc of analyticity near the resonant Bloch parameter.

In Fig. 1 two resonant curves are marked; a quartet resonance is marked with plus signs and a quintet is marked with circles. The quartet curve includes Class I instability [10] for $H \in (0.855, 1)$. The leading order growth rate of this instability, λ_2, is plotted in Fig. 3. The quintet resonance, marked with circles in Fig. 1, is a collision of eigenvalues with opposite Krein signature but does not lead to instability. Note that this statement on stability is in the context of the TFE method, where the spectrum is computed with the fixed Bloch parameter. Based on our investigations of the radius of convergence near these Bloch parameters, we believe that the quintet configurations do lead to instability, but that the Bloch parameters where these instabilities occur do not include the resonant Bloch parameters, at which there was an eigenvalue collision at zero amplitude.

Close-ups of the radius of the disc of analyticity near two resonant Bloch parameters are given in Fig. 4. The Bloch parameters are chosen to reflect the typical observed behavior when the resonant Bloch parameter includes an analytic instability, as on the left, and where the resonant Bloch parameter has pure imaginary spectrum within its disc of analyticity, as on the right. In both cases our asymptotic approximation predicts a collision of opposite Krein signature eigenvalues which vanishes like the square root of p for $p > p_{crit}$. Numerical estimates of the radius of the disc of analyticity imply that in the unstable case, the left panel of Fig. 4, the spectrum loses analyticity in both the left- and right-hand limits of the resonant Bloch parameter. In the right panel, where the resonant configuration had a pure imaginary spectrum, the disc of analyticity did not vanish as the resonant Bloch parameter is approached from the left. Thus we expect finite amplitude instabilities to exist in bands of Bloch parameters which include the resonant case, as in the left panel, or do not, as in the right panel. In other words, as the amplitude increases the bands of unstable Bloch parameters both grow in width and move in location. The support of these bands may or may not include the resonant Bloch parameters from the zero amplitude case. The TFE method only computes the spectrum with fixed Bloch parameter, and thus cannot compute the spectrum within these bands, except at the resonant Bloch parameters.

Based on our results we believe that there are many finite amplitude instabilities which cannot be computed by the TFE method. These instabilities exist in bands of Bloch parameters which move as the wave amplitude increases. If the band includes the resonant Bloch parameter at finite amplitude, then the TFE method computes the unstable spectrum at this Bloch parameter, as in the left panel of Fig. 4, and provides a predicted location of the band. If the band does not include the resonant Bloch parameter at finite amplitude, then the TFE method does not compute any instability. Instead it provides a predicted location of the band of unstable Bloch parameters, as in the right of Fig. 4. An instability has recently been computed by Deconinck and Trichtchenko whose location agrees with this interpretation [37].

3.4. Comparison with other results

Such an expansion (essentially expanding p as a function of ε) has been successfully applied to compute near-resonant traveling waves to the KdV equation [39]; the leading order asymptotics of the spectrum are derived with a multi-scale expansion for deep-water gravity–capillary waves in [26]. A multi-scale extension of the TFE method presented here should be able to compute the finite amplitude instabilities in the neighborhood of the configurations in Fig. 4.

Apart from the marked resonance curves in Fig. 1, the spectrum also loses analyticity near $p = 0$, for $H > 1.363$. This is due to the Benjamin–Feir instability, a collision of flat state eigenvalues of algebraic multiplicity four, which is not currently supported by the algorithm [27]. Extending the algorithm to higher dimensional null spaces is not sufficient to compute this instability; however, as for fixed p the instability is either not present ($p = 0$) or not analytic in ε (for p small). In order to compute these bands of instability via boundary perturbation, the method must allow the Bloch parameter to depend on amplitude, as is not done here. The analyticity of the spectrum for Bloch parameters which depend on amplitude is an open question.

In the recent work of Oliveras & Deconinck [13], unstable sections of the spectrum were reported at $H = 0.5$ with $\varepsilon = 0.01$, see their Figure 9(b), near $\lambda \approx 0.1489i$ and $\lambda \approx 0.5212i$. The two eigenvalues are in the neighborhood of the aforementioned quartet and quintet configurations respectively. In both cases, our computations indicate that the spectrum is pure imaginary. Thus the instability of Oliveras & Deconinck is not analytic in amplitude for fixed p. Instead, these instabilities occur in bands of Bloch parameters which both move as a function of amplitude and do not include the resonant Bloch parameter at finite amplitude.

The structure of the set of resonances of the spectrum of traveling waves in the potential flow equations (1) is quite rich. In addition to the resonances mentioned in the previous paragraphs, the equation supports non-isolated resonances, at which λ_0 has kernel of dimension higher than two. Non-isolated resonances (e.g., where a wavenumber is part of both a triad *and* a quartet), create the "rough" regions in Fig. 1. We note that these non-isolated resonances accumulate in the region $H \leq 0.5$. It is not clear that an amplitude expansion is the right approach to compute the spectrum in a region where the resonant sets are intertwined in such a complicated manner.

4. Conclusion

A perturbative numerical method was presented for computing simple and resonant spectra for finite depth gravity waves, extending the previous work from infinite depth. This method computes the analytic spectrum for fixed Bloch parameter p and can be used to numerically approximate the radius of the disc of analyticity of the spectrum. The leading order asymptotics of the spectrum are also directly calculated and compared with these numerical results. An instability is observed to be analytic in amplitude, with fixed Bloch parameter, for $kh \in (0.855, 1)$. Elsewhere the spectrum is either pure imaginary or not analytically connected to the flat state. A modulational extension of this method, which expands the Bloch parameter in ε, will allow for the computation of instabilities which depend nontrivially on the Bloch parameter, and is currently being pursued, based on recent multi-scale asymptotics of the spectrum of deep-water gravity–capillary waves [26].

Acknowledgments

The authors would like to thank B. Deconinck and O. Trichtchenko for valuable discussions, including access to unpublished results. These discussions both improved the authors understanding of the results herein, as well as led to increased perspective on the global stability picture. DPN gratefully acknowledges the support from the National Science Foundation through Grant No. DMS-1115333, and the Department of Energy under Award No. DE-SC0001549.

References

[1] F. Dias, C. Kharif, Nonlinear gravity and gravity-capillary waves, Annu. Rev. Fluid Mech. 31 (1999) 301–346.
[2] A.D.D. Craik, George Gabriel Stokes on water wave theory, Annu. Rev. Fluid Mech. 37 (2005) 23–42.
[3] L.F. McGoldrick, An experiment on second-order capillary gravity resonant wave interactions, J. Fluid Mech. 40 (1970) 251–271.
[4] J. Reeder, M. Shinbrot, Three dimensional, nonlinear wave interaction in water of constant depth, Nonlinear Anal. 5 (1981) 303–323.
[5] D.P. Nicholls, F. Reitich, Stable, high-order computation of traveling water waves in three dimensions, Eur. J. Mech. B Fluids 25 (2006) 406–424.
[6] T.B. Benjamin, J.E. Feir, The disintegration of wave trains on deep water, J. Fluid Mech. 27 (1967) 417–430.
[7] O.M. Phillips, On the dynamics of unsteady gravity waves of finite amplitude. Part 1. The elementary interactions, J. Fluid Mech. 9 (1960) 193–217.
[8] D.J. Benney, Non-linear gravity wave interactions, J. Fluid Mech. 14 (1962) 577–584.
[9] J.L. Hammack, D.M. Henderson, Resonant interactions among surface water waves, Annu. Rev. Fluid Mech. 25 (1993) 55–97.
[10] R.S. MacKay, P.G. Saffman, Stability of water waves, Proc. R. Soc. Lond. Ser. A 406 (1986) 115–125.
[11] J. McLean, Instabilities of finite-amplitude gravity waves on water of finite depth, J. Fluid Mech. 114 (1982) 331–341.
[12] J. McLean, Y.C. Ma, D.U. Martin, P.G. Saffman, H.C. Yuen, Three-dimensional instability of finite-amplitude water waves, Phys. Rev. Lett. 46 (1981) 817–820.
[13] B. Deconinck, K. Oliveras, The instability of periodic surface gravity waves, J. Fluid Mech. 675 (2011) 141–167.
[14] M.S. Longuet-Higgins, The instabilities of gravity waves of finite amplitude in deep water. I. Superharmonics, Proc. R. Soc. Lond. Ser. A 360 (1703) (1978) 471–488.
[15] M.S. Longuet-Higgins, The instabilities of gravity waves of finite amplitude in deep water. II. Subharmonics, Proc. R. Soc. Lond. Ser. A 360 (1703) (1978) 489–505.
[16] M. Francius, C. Kharif, On the disappearance of the lowest-order instability for steep gravity waves in finite depth, Phys. Fluids 15 (2003) 2445.
[17] M. Francius, C. Kharif, Three-dimensional instabilities of periodic gravity waves in shallow water, J. Fluid Mech. 561 (2006) 417–437.
[18] O. Kimmoun, M. Ioualalen, C. Kharif, Instabilities of steep short-crested surface waves in deep water, Phys. Fluids 11 (1999) 1679.

[19] D.P. Nicholls, Spectral stability of traveling water waves: analytic dependence of the spectrum, J. Nonlinear Sci. 17 (4) (2007) 369–397.
[20] D.P. Nicholls, F. Reitich, On analyticity of traveling water waves, Proc. R. Soc. Lond. Ser. A 461 (2057) (2005) 1283–1309.
[21] D.P. Nicholls, J. Shen, A rigorous numerical analysis of the transformed field expansion method, SIAM J. Numer. Anal. 47 (4) (2009) 2708–2734.
[22] D.P. Nicholls, Spectral data for traveling water waves : singularities and stability, J. Fluid Mech. 624 (2009) 339–360.
[23] D.P. Nicholls, Spectral stability of traveling water waves: Eigenvalue collision, singularities, and direct numerical simulation, Physica D 240 (4–5) (2011) 376–381.
[24] B. Akers, D.P. Nicholls, Spectral stability of deep two-dimensional gravity water waves: repeated eigenvalues, SIAM J. Appl. Math. 72 (2012) 689–711.
[25] B. Akers, D.P. Nicholls, Spectral stability of deep two-dimensional gravity capillary water waves, Stud. Appl. Math. 130 (2013) 81–107.
[26] B. Akers, Modulational stability of water waves. Preprint.
[27] B. Akers, D.P. Nicholls, Traveling waves with gravity and surface tension, SIAM J. Appl. Math. 70 (2010) 2373–2389.
[28] B. Akers, The generation of capillary–gravity solitary waves by a surface pressure forcing, Math. Comput. Simulation 82 (2012) 958–967.
[29] N.A. Phillips, A coordinate system having some special advantages for numerical forecasting, J. Atmospheric Sci. 14 (2) (1957) 184–185.
[30] J. Chandezon, D. Maystre, G. Raoult, A new theoretical method for diffraction gratings and its numerical application, J. Opt. 11 (7) (1980) 235–241.
[31] A. Mielke, Instability and stability of rolls in the Swift–Hohenberg equation, Comm. Math. Phys. 189 (3) (1997) 829–853.
[32] B. Deconinck, J.N. Kutz, Computing spectra of linear operators using the Floquet–Fourier–Hill method, J. Comput. Phys. 219 (2006) 296–321.
[33] A. Davey, K. Stewartson, On three-dimensional packets of surface waves, Proc. R. Soc. Lond. A. Math. Phys. Sci. 338 (1613) (1974) 101–110.
[34] H. Hasimoto, H. Ono, Nonlinear modulation of gravity waves, J. Phys. Soc. Japan 33 (3) (1972) 805–811.
[35] G.B. Whitham, Linear and Nonlinear Waves, Wiley, 1974.
[36] A.D.D. Craik, Wave Interactions and Fluid Flows, Cambridge University Press, 1985.
[37] B. Deconinck, O. Trichtchenko, Personal Communication, 2013.
[38] K. Hasselmann, A criterion for nonlinear wave stability, J. Fluid Mech. 30 (1967) 737–739.
[39] S.E. Haupt, J.P. Boyd, Modeling nonlinear resonance: a modification of the Stokes perturbation expansion, Wave Motion 10 (1988) 83–98.